sponding resonances for **3** (+81.9 and +99.8 ppm) (*7*) and **5** (+97.7 ppm) (*8*). The Si_u resonances were well reproduced in the pertinent model compounds by ab initio MO calculations; the resonances were +178.3, +105.3, and +110.1 ppm for **6** (D_{2d}), spiropentasilene **8** (C_{2v}), and cyclotrisilene **11** (C_{2v}) at the GIAO/B3LYP/6-311+G(2*df*,*p*)//B3LYP/6-31G(*d*) level. Because the Si_u resonances in various disilenes are related to the reciprocal of the energy difference between σ and π* orbitals of the Si=Si bond (*26*), the remarkable lower-field shift of the Si_u resonance in **2** may be taken as another indication for the pronounced through-space interaction between π* orbitals. Unfortunately, the resonance due to the central ^{29}Si nucleus in **2** was not observed, probably as a result of the large spin-lattice relaxation time; the corresponding resonance in **6** was found at −45.9 ppm by the GIAO calculations (*16*).

The successful isolation of a spiropentasiladiene encourages us to make new types of silicon unsaturated compounds with new properties. Studies of the chemistry of these compounds may be an important innovation in the theory of chemical bonding and reactivity.

References and Notes

1. R. West, M. J. Fink, J. Michl, *Science* **214**, 1343 (1981).
2. G. Raabe, J. Michl, in *The Chemistry of Organic Silicon Compounds*, S. Patai, Z. Rappoport, Eds. (Wiley, New York, 1989), part 2, chap. 17.
3. T. Tsumuraya, S. A. Batcheller, S. Masamune, *Angew. Chem. Int. Ed. Engl.* **30**, 902 (1991).
4. R. Okazaki, R. West, *Adv. Organomet. Chem.* **39**, 231 (1996).
5. M. Kira, T. Iwamoto, C. Kabuto, *J. Am. Chem. Soc.* **118**, 10303 (1996).
6. N. Wiberg, H. Auer, H. Nöth, J. Knizek, K. Polborn, *Angew. Chem. Int. Ed. Engl.* **36**, 2869 (1998).
7. T. Iwamoto, C. Kabuto, M. Kira, *J. Am. Chem. Soc.* **121**, 886 (1999).
8. M. Ichinohe, T. Matsuno, A. Sekiguchi, *Angew. Chem. Int. Ed. Engl.* **37**, 2194 (1999).
9. A. Grybat, S. Boomgaaden, W. Saak, H. Marsmann, M. Weidenbruch, *Angew. Chem. Int. Ed. Engl.* **38**, 2010 (1999).
10. M. Weidenbruch, S. Willms, W. Saak, G. Henkel, *Angew. Chem. Int. Ed. Engl.* **36**, 2503 (1997).
11. A saturated spiropentasilane has been reported [P. Boudjouk, R. Sooriyakumaran, *J. Chem. Soc. Chem. Commun.* 777 (1984)].
12. W. E. Billups, M. M. Haley, *J. Am. Chem. Soc.* **113**, 5084 (1991).
13. R. K. Saini, V. A. Litosh, A. D. Daniels, W. E. Billups, *Tetrahedron Lett.* **40**, 6157 (1999).
14. The detailed formation mechanism for **2** is currently under investigation. **2**: oxygen- and moisture-sensitive dark red crystals; melting point, 216° to 218°C; ^1H NMR (C_6D_6, δ): 0.68 (*s*, 72 H), 1.18 (*s*, 108 H); ^{13}C NMR (C_6D_6, δ): 2.5, 20.4, 29.5; ^{29}Si NMR (C_6D_6, δ): −100.6, 6.7, 154.2 (the resonance for the central silicon was not observed); UV-visible (3-methylpentane) λ_{max} (in nanometers) ($\varepsilon/10^4$): 560 (0.253), 500 (0.364), 428 (1.17), 383 (1.81), 304 (8.70), 265 (6.61, *sh*), 250 (8.63, *sh*), 235 (7.78, *sh*).
15. A single crystal of **2** used for the collection of x-ray diffraction involved two hexane molecules as a cosolvent for each spiropentasiladiene. Crystal data for **2**: $[C_{72}H_{180}Si_{21}\cdot(C_6H_{14})_2]$, formula weight = 1808.36; dark red plate; orthorhombic; space group = I_{bca}; cell constants, a = 27.510(3) Å, b = 29.461(1) Å, c = 29.830(1) Å; V (cell volume) = 24175(2) $Å^3$; number of molecules per unit cell (Z) = 8; calculated density (D_{calcd}) = 0.994 g/cm^3. Intensities of reflections were collected on a Rigaku/MSC Mercury charge-coupled device diffractometer with a graphite monochromated Mo-Kα radiation (λ = 0.71069 Å) at 150 K. Of the 79,057 reflections that were collected, 14,416 were unique. The structure was solved by direct methods and refined anisotropically for nonhydrogen atoms. Hydrogen atoms and carbon atoms of a solvent were included but not refined. The final cycle of full-matrix least-squares refinement was based on 4943 observed reflections [$I > 2.00\sigma(I)$, where I is the observed reflection intensity] and 420 variable parameters and converged with unweighted and weighted agreement factors of R = 0.066, R_w = 0.078, and GOF (goodness of fit) = 1.51. All calculations were performed with the teXsan crystallographic software package of Molecular Structure Corporation. Coordinates and other crystallographic information will be deposited in the Cambridge Crystallographic Database (*16*).
16. Supplementary data are available at *Science* Online at www.sciencemag.org/feature/data/1052253.shl.
17. M. J. Frisch *et al.*, *GAUSSIAN 98 (Revision A.7)* (Gaussian, Pittsburgh, PA, 1998).
18. L. Nyulászi, P. v. R. Schleyer, *J. Am. Chem. Soc.* **121**, 6872 (1999).
19. A. Goller, H. Heydt, T. Clark, *J. Org. Chem.* **61**, 5840 (1996).
20. For a recent example of the σ*-aromaticity in silacyclopropenes, see S. Tsutsui, K. Sakamoto, C. Kabuto, M. Kira, *Organometallics* **17**, 3819 (1998).
21. A homodesmotic reaction is defined as a reaction in which (i) there are equal numbers of C (or Si) atoms in their various states of hybridization in reactants and products and (ii) there are equal numbers of C (or Si) atoms with zero, one, two, and three H atoms attached in reactants and products (*27*). A homodesmotic reaction is arbitrarily chosen, but SE was almost independent of the choice. Several authors have calculated SE values for the parent spiropentadiene. Typically, the SE value was reported to be 117.7 kcal/mol when the same Eq. 2 at the 4-31G level was used (*22*). The SE values for spiropentadiene and related compounds calculated at the B3LYP/6-311++G(3*df*,2*p*)//B3LYP/6-31G(*d*) level are given in the supplementary material (*16*). As expected, the SE values of the spiro compounds are approximately equal to the sums of those of the component three-membered ring compounds. The SE value of the parent cyclotrisilene (34.5 kcal/mol) is similar to that of cyclotrisilane (35.5 kcal/mol), whereas the SE value of cyclopropene (55.5 kcal/mol) is 20 kcal/mol larger than that of cyclopropane (25.5 kcal/mol). Thus, the SE values of the parent spiropentasilane [10 (D_{2d})], spiropentasilene [9 (C_{2v})], and spiropentasiladiene [7(D_{2d})] are similar (60 to 70 kcal/mol) to each other, whereas those of the corresponding carbon compounds depend notably on the number of double bonds; the SE values are 55.5, 85.7, and 114.2 kcal/mol for spiropentane, spiropentene, and spiropentadiene, respectively.
22. J. Kao, L. Radom, *J. Am. Chem. Soc.* **100**, 766 (1978).
23. H. E. Simmons, T. Fukunaga, *J. Am. Chem. Soc.* **89**, 5208 (1967).
24. R. Hoffmann, A. Imamura, G. D. Zeiss, *J. Am. Chem. Soc.* **89**, 5215 (1967).
25. The CIS (configuration interaction, singlet) calculations for **7** (D_{2d}) [CIS/6-311++G(3*df*,2*p*)//B3LYP/6-31G(*d*)] predicted two degenerate π→π* bands at 358 and 293 nm, in addition to two π→σ* (a_1) and other transitions with negligible intensities in the UV-visible region; the π→π* band maximum for cyclotrisilene 12 (C_{2v}) was calculated to be 344 nm. As expected, the CIS calculations predicted that the distortion of **7** (D_{2d}) to **7** (D_2) caused the splitting of the degenerate two π→π* bands as well as the remarkable red shift of the longest wavelength band. For **7** (D_2), four band maxima of 422, 353, 288, and 283 nm with moderate intensities were found in the UV-visible region, where three of them were π→π* bands, but the 288-nm band showed a strong π→σ* nature (*16*). More sophisticated calculations on the real molecule are desirable for the convincing assignment of the absorption bands of **2**.
26. R. West *et al*, *J. Am. Chem. Soc.* **119**, 4972 (1997).
27. P. George, M. Trachtman, C. W. Bock, A. M. Brett, *Tetrahedron* **32**, 317 (1976).

28. We thank an anonymous reviewer for helpful discussion. Supported by the Ministry of Education, Science, Culture, and Sports of Japan [Grants-in-Aid for Scientific Research on Priority Areas (A) "The Chemistry of Inter-element Linkage" No. 09239101 (M.K.), Scientific Research (B) No.11440185 (M.K. and T.I.), and Encouragement of Young Scientists No. 12740336 (T.I.)].

16 May 2000; accepted 13 September 2000

Dimer Preparation That Mimics the Transition State for the Adsorption of H_2 on the Si(100)-2 × 1 Surface

Emily J. Buehler and John J. Boland*

A chemically induced dimer configuration was prepared on the silicon (Si) (100) surface and was characterized by scanning tunneling microscopy (STM) and spectroscopy (STS). These prepared dimers, which are essentially untilted and differ both electronically and structurally from the dynamically tilting dimers normally found on this surface, are more reactive than normal dimers. For molecular hydrogen (H_2) adsorption, the enhancement is about 10^9 at room temperature. There is no appreciable barrier for the H_2 reaction at prepared sites, indicating the prepared configuration closely approximates the actual dimer structure in the transition state. This previously unknown ability to prepare specific surface configurations has important implications for understanding and controlling reaction dynamics on semiconductor surfaces.

The reaction of H_2 with the Si(100)-2 × 1 surface is perhaps the best characterized and most important adsorbate-semiconductor system (*1*), but even the dynamics of H_2 on Si(100)-2 × 1 are poorly understood. Repeated experiments have shown that the barrier to the recombination of H atoms and subsequent desorption of H_2 is 2.5 eV (*2*), whereas the bond energies of the Si-H reactants and H-H product are ~3.5 and 4.5 eV (*3*), respectively. Together, these results suggest the absence of a significant barrier to adsorption (Fig. 1). State-resolved gas-phase studies show that H_2 product molecules gain little excess translational energy when they leave the surface, which is consistent with a small barrier in the adsorption channel (*4*, *5*). However, direct adsorption studies measure a sticking coefficient below 10^{-13} at room temperature and a barrier to adsorption of 0.7 eV (*6*, *7*).

These observations cannot be reconciled by considering exclusively the dynamics of incident H_2 molecules on the Si(100) surface (*4*, *5*, *8*). Instead, motivated by the observation of increased sticking probability at higher surface temperatures, recent theoretical studies have focused on the role of the surface itself (*7*, *9–11*). The dimer units that compose the bare Si(100) surface tilt back and forth in a low-frequency (~5 THz) seesaw mode (*12*). In contrast, dimers that have reacted with H_2 have their Si-Si dimer bonds slightly elongated and locked in the horizontal plane of the surface (*3*, *13*, *14*). The existing data seem to support a "late" transition state (one that looks more like the product state) for adsorption involving a dimer configuration that is better approximated by a reacted horizontal dimer than a bare tilted dimer (*7*). Enhanced sticking reported at elevated temperatures therefore results from the increased probability of exciting a bare dimer into a more horizontal configuration.

Motivated by these insights, we describe here the use of surface chemistry to prepare a population of distinctive dimer sites and to investigate their properties and reactivity toward H_2 using STM and STS. Specifically, we create and characterize bare dimers that are essentially untilted such that their dimer bonds are constrained to the horizontal surface plane. The room-temperature H_2 sticking coefficient at these untilted dimer sites is a factor of 10^9 greater than that measured at tilting dimer sites. The measured sticking coefficient is also insensitive to the surface temperature, which indicates that the untilted dimer configuration is optimized and thus a reasonable approximation to the actual transition state geometry.

To prepare and characterize untilted dimer sites, a Si(100)-2 × 1 surface was exposed to a submonolayer coverage ($\theta = 0.05$) of H atoms and then subsequently annealed to 600 K for up to 180 s. (*15*) Figure 2A shows the presence of bright ball-like features and dark dimers on an otherwise unreacted surface. The former (latter) represent dimers that have reacted with one (two) H atoms, i.e., half-filled and filled dimers, respectively. H-filled dimers are symmetric with Si-Si dimer bonds fixed in the horizontal surface plane. The arrow in Fig. 2A identifies an untilted dimer that is located in the same row next to dimers that are H-filled. Untilted dimers are unreacted but better resolved than surrounding bare dimers. This difference in appearance is, at least in part, the result of an elastic strain-field induced by neighboring H-filled sites that constrains the dimer bond to the horizontal plane.

The presence of this strain-field is more apparent in the low-temperature images in Fig. 2, B and C. In regions not containing H-filled dimer sites, the surface forms local c(4 × 2) domains that consist of anticorrelated patterns of tilted dimers—the ground-state structure of the bare Si(100) surface (*16*). However, dimers next to H-filled dimers remain untilted, and this effect extends for many dimers on either side of the H-filled dimers. To eliminate the possibility that the neighboring untilted dimers are dynamically tilting on a time scale that is inaccessible to STM, we imaged the surface at temperatures down to ~20 K. It was not possible to induce the neighboring dimers to tilt even under these low-temperature conditions. The persistence length of the strain-field on either side of the H-filled dimers remained unchanged (15 to 20 dimers) over the entire temperature range studied (20 to 200 K). Larger, more controlled populations of untilted dimers could be produced by desorbing small amounts [0.001 monolayer (ML)] of H_2 from a Si(100)-2 × 1 surface that has been completely reacted with H atoms. In this case, bare, untilted dimers were surrounded on all sides by H-filled dimers. Figure 2D shows a population of bare, untilted dimers; they are easily identified in empty-state images by the presence of a nodal feature across the middle of the dimer.

Figure 3A compares room-temperature STS spectra measured at tilted and untilted

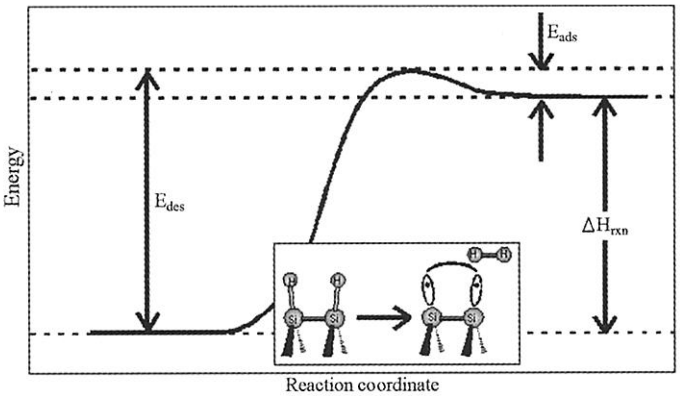

Fig. 1. Potential energy diagram for H_2 on Si(100) that shows the relation between the heat of reaction (ΔH_{rxn}) and the barriers to desorption (E_{des}) and adsorption (E_{ads}). The bond energies and known value of E_{des} suggest that E_{ads} is small, consistent with state-resolved measurements of the H_2 desorption product. Inset, diagram of reactants and products that occur during the reaction.

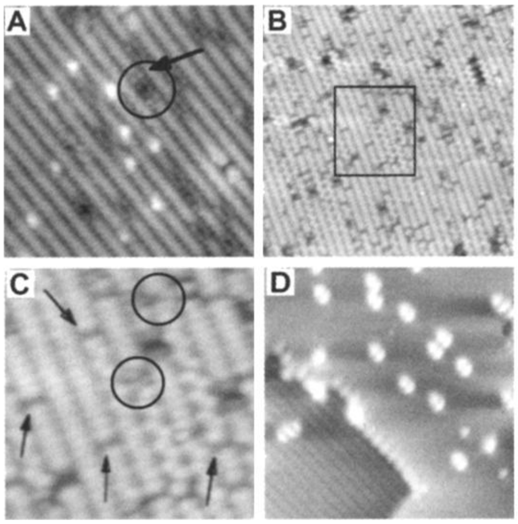

Fig. 2. (**A**) Empty-state image of clean Si(100)-2 × 1 partially dosed with H atoms and then heated to allow H diffusion and pairing. Image is ~14 nm by 14 nm and was recorded at −0.8 V. Dimers containing one H atom appear as bright spots; those with two Hs are darkened. The bare dimers located next to H-filled dimers are resolved into two atoms. (**B**) Filled-state image of the surface cooled to ~200 K. Image is ~23 nm by 23 nm and was taken at +1.6 V. Rows of ordinary bare dimers are pinned into c(4 × 2) domains. Several rows of untilted dimers are seen due to the presence of H-filled dimers. Box, area shown in (C). (**C**) Close up of the box in (B). Several H-filled dimers are indicated by arrows, and C defects are circled. H-filled dimers pin neighboring dimers into an untilted configuration. The extent of pinning is limited by the presence of C defects that pin neighboring dimers in a tilted configuration. Filled-state images are presented to show the buckling of the dimers, but they do not resolve individual atoms of a dimer. (**D**) Empty-state image of Si(100)-2 × 1:H, heated to allow a small amount of H_2 to desorb. Image is ~19 nm by 19 nm and was taken at −1.7 V. Bare, untilted dimers appear as bright spots; the node of the antibonding orbital is visible on the middle of each bare dimer, making it easy to identify.

Venable and Kenan Laboratories, Department of Chemistry, University of North Carolina at Chapel Hill, Chapel Hill, NC 27599–3290, USA.

*To whom correspondence should be addressed. E-mail: boland@unc.edu

dimer sites. Tilted dimers show a small superstructure band gap characteristic of the energy splitting between the filled and empty states localized at the tilted-up ends and tilted-down ends of dimers, respectively (*1*, *17*). Untilted dimer sites have a different signature: A distinct pair of empty and filled states separated by an energy of 2.4 eV. Analysis of this spectrum is complicated by tip-induced band bending on the H-reacted surface. Band-bending effects can be estimated from the H-filled dimer spectrum in Fig. 3A; the energy gap is 1.5 eV instead of 1.1 eV (*17*), indicating a 25% voltage drop in the Si. We attribute the (corrected) 1.8-eV energy gap to a π-π^* interaction of the dangling bonds at untilted dimer sites. The magnitude of this energy splitting is greater than that found for a surface comprised of interacting dimers but consistent with calculations for a single isolated symmetric dimer (*18*).

The reactivity of untilted dimer sites to H_2 was measured directly by STM. Figure 3, B and C, show the Si(100) surface before and after H_2 adsorption. Circles indicate the locations of bare untilted dimers on the surface; the number of such sites decreases noticeably following H_2 adsorption. By analyzing the change in the untilted dimer population before and after H_2 exposure, the reactivity of untilted dimers was measured in terms of an effective sticking coefficient S_{eff} defined by

$$S_{\text{eff}} = (-\Delta\theta/\Delta t)/Z \tag{1}$$

Here, $\Delta\theta$ is the relative change in the untilted dimer population during an H_2 dose of time Δt, and $Z = P/(2\pi m_{H_2} kT)^{1/2}$ is the rate of H_2 molecules (with mass m_{H_2}) incident on the surface at pressure P, where k is Boltzmann's constant and T is temperature. Figure 3D shows the measured values of S_{eff} over a range of surface temperatures (77 to 520 K). Also plotted is the sticking coefficient on the bare surface measured by Bratu *et al.* using second harmonic generation (*6*). The S_{eff} measured at untilted dimer sites is nine orders of magnitude greater than that on the bare surface. Moreover, the temperature dependence of the sticking coefficient is dramatically reduced compared with the bare surface, indicating there is little need to excite untilted dimers into a suitable configuration for reaction.

Other low-barrier adsorption pathways have been reported and involve step sites (*19*) or half-filled interdimer sites (*20*); the latter were also generated by a pre-exposure to H atoms. The relative importance of these pathways has not been established. The intradimer pathway described here will be important at high coverages or at high temperatures (>500 K) where there is a thermodynamic driving force for the formation of H-filled dimers (*17*). The sticking coefficient reported for the bare surface (*6*) includes contributions from all possible sites (inter- as well as intradimer sites) so that the actual room-temperature enhancement at intradimer sites may be greater than 10^9.

Figure 4 shows a qualitative potential energy surface that summarizes the results of this report and incorporates some of the detailed aspects of the dynamics revealed by recent experimental (*4*, *5*, *8*) and theoretical studies (*7*, *9–11*). Molecular adsorption at tilted sites involves excitation from the minimum of the double-well potential, which characterizes the internal tilting coordinate of the dimer. The enhancement in the sticking coefficient at elevated temperatures then results from an increased probability of finding the dimer in a less tilted configuration. The barrier for adsorption at untilted sites involves excitations from regions close to the maximum of the double-well potential and is correspondingly smaller than that at tilted sites. Because untilted sites have a minimal barrier to reaction, the untilted dimer configuration is optimized and close to the actual transition state geometry. On the basis of this, the transition state for H_2 adsorption on a Si(100) dimer is late or product-like. Correspondingly, the transition state for H_2 desorption from a dimer must be early, and the departing molecule is only weakly accelerated along the molecule-surface coordinate, consistent with state-resolved measurements of the H_2 desorption product (*4*). However, energy is redistributed into the internal tilting coordinate as the dimer flips from the untilted geometry of the transition state to the tilted geometry of the bare surface.

These results raise several important issues. First, because the presence of hydrogen-filled dimers promotes adsorption of further hydrogen the adsorption process should be autocatalytic, which is consistent with recent measurements (*21*). A second issue concerns the absence of any significant barrier to adsorption at untilted sites. The Si(100) dimers tilt dynamically at room temperature, so the barrier between the double wells in Fig. 4 is substantially less than the 0.7-eV value associated with adsorption. If adsorption involves single dimer sites, then a possible explanation is that the 0.7-eV value is the energy required or gained from tilting not a single dimer but rather a domain of dimers. This interpretation is consistent with the data in Fig. 2, which show the importance of long-range correlations on this surface. In this sense, it might be more appropriate to view this barrier as a dynamical bottleneck that is the result of a highly constrained transition state. Lastly, symmetry arguments suggest that the dimer is in an electronically excited state immediately after H_2 desorption (*22*). The excited state

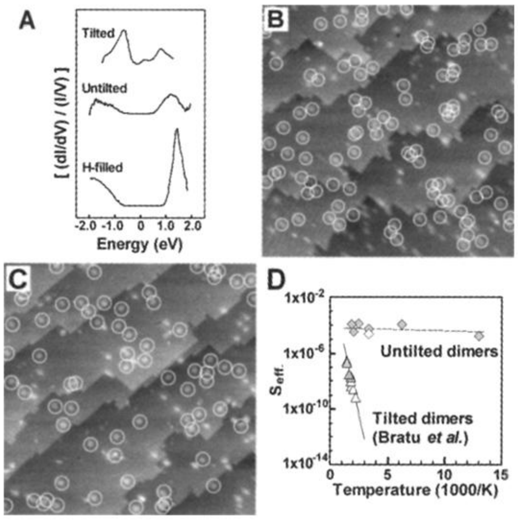

Fig. 3. (**A**) STS curves taken over bare, tilted dimers; bare, untilted dimers; and H-filled dimers on the Si(100) surface. Each curve is the average of STS curves taken at several sites. The range of energies probed was limited (–2 V to +2 V) to avoid tip-induced desorption that occurs at high biases. (**B** and **C**) Empty-state images of a larger area of the surface before and after H_2 dosing. Each image is ~46 nm by 46 nm and was taken at −2.2 V (B) or −2.0 V (C). The entire population of bare, untilted dimers has been circled; other white features are mainly dimers containing single H atoms produced by H-atom diffusion during and after the preparation step (Fig. 2A). The population of bare, untilted dimers decreases noticeably with molecular H_2 dosing. (**D**) Arrhenius plot of the effective sticking coefficient (S_{eff}) versus inverse temperature for H_2 (open symbols) and D_2 (gray symbols) on Si(100). Measured values for the bare, tilted dimers [Bratu *et al.* (*6*)] are shown for comparison and have an associated barrier of 0.7 eV.

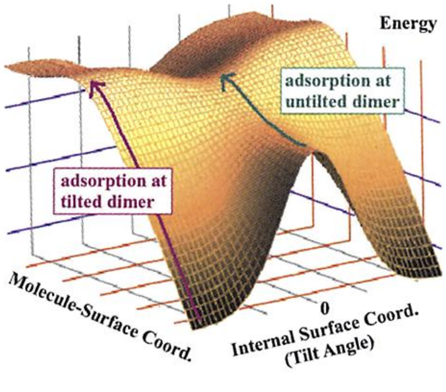

Fig. 4. Qualitative potential energy surface for the adsorption of H_2 at a Si(100) dimer site. The barrier to adsorption at a tilted dimer is much greater than that at an untilted dimer. The effective barrier is in the internal tilting coordinate of the surface and not in the molecule-surface coordinate.

lifetime and the relaxation process to the ground state are not known, and either may account for the enhanced reactivity at untilted dimer sites.

The ability to prepare dimers on a Si(100) surface has implications beyond the present system. There are many surface reactions that yield a range of unexpected products. The product distribution may reflect the dynamics of the surface atoms involved, and the detailed mechanisms of such reactions may be studied by the present method. Although untilted dimer sites can be generated by adsorption of other species such as halogens, the use of hydrogen is particularly attractive. Hydrogen is both small and electroneutral, so that other than pinning the geometry at adjacent dimer sites, it does not unduly influence the chemistry that takes place at these sites. This method is also likely to be important for other semiconductor systems because the charge density on these surfaces will generally be insufficient to screen chemically induced lattice distortions from neighboring sites.

References and Notes

1. D. J. Doren, *Adv. Chem. Phys.* **95**, 1 (1996).
2. M. L. Wise, B. G. Koehler, P. Gupta, P. A. Coon, S. M. George, *Surf. Sci.* **258**, 166 (1991).
3. Z. Jing, J. L. Whitten, *J. Chem. Phys.* **98**, 7466 (1993).
4. K. W. Kolasinski, W. Nessler, A. Meijere, E. Hasselbrink, *Phys. Rev. Lett.* **72**, 1356 (1994).
5. K. W. Kolasinski, W. Nessler, K. Bornscheuer, E. Hasselbrink, *J. Chem. Phys.* **101**, 7082 (1994).
6. P. Bratu, K. L. Kompa, U. Hofer, *Chem. Phys. Lett.* **251**, 1 (1996).
7. P. Bratu *et al.*, *Phys. Rev. B* **54**, 5978 (1996).
8. K. W. Kolasinski, S. F. Shane, R. N. Zare, *J. Chem. Phys.* **96**, 3995 (1992).
9. E. Pehlke, M. Scheffler, *Phys. Rev. Lett.* **74**, 952 (1995).
10. P. Kratzer, B. Hammer, J. K. Nørskov, *Chem. Phys. Lett.* **229**, 645 (1994).
11. W. Brenig, A. Gross, R. Russ, *Z. Phys. B* **96**, 231 (1994).
12. P. C. Weakliem, G. W. Smith, E. A. Carter, *Surf. Sci. Lett.* **232**, L219 (1990).
13. M. R. Radeke, E. A. Carter, *Phys. Rev. B* **54**, 11803 (1996).
14. E. M. Lauridsen *et al.*, *Surf. Sci.* **453**, 18 (2000).
15. Experiments were carried out in an Omicron Variable Temperature STM (VT-STM) system that has a base pressure of $\sim 5 \times 10^{-11}$ torr. The STM was operated in constant current mode with the tunneling bias applied to the tip. Images were recorded at +2 V and −2 V, voltages low enough to ensure that the tip did not induce hydrogen desorption (*23*). Sample cooling was accomplished by pumping liquid N_2 or He through a continuous flow cryostat that was thermally coupled to the sample via a copper braid and clamping mechanism. Clean Si(100)-2 × 1 surfaces were prepared by heating the Si(100) substrate (1ohm-cm, phosphorus doped) to ~1350 K to desorb the native oxide and were then cooled slowly to form a good 2 × 1 reconstruction. Hydrogen-passivated Si(100)-2 × 1 surfaces were prepared by dosing the clean surface with atomic hydrogen while the substrate temperature was held at ~600 K. Molecular adsorption experiments were performed using both hydrogen and deuterium, with similar results. The dosing gas was cooled by liquid N_2 before dosing to remove all traces of reactive contaminants (primarily H_2O). Dosing was performed by backfilling the preparation chamber with room-temperature H_2 or D_2 to a pressure of 5.0×10^{-7} torr. All ion pumps and filaments were turned off, and the exposures described were corrected for the detection efficiency of H_2.
16. R. A. Wolkow, *Phys. Rev. Lett.* **68**, 2636 (1992).
17. J. J. Boland, *Phys. Rev. Lett.* **67**, 1539 (1991).
18. J. E. Northrup, *Phys. Rev. B* **47**, 10032 (1993). This paper describes an energy gap of about 1 eV, but the method used underestimates the true gap by at least 0.5 eV.
19. P. Kratzer, E. Pehlke, M. Scheffler, M. B. Raschke, U. Hofer, *Phys. Rev. Lett.* **81**, 5596 (1998).
20. A. Biedermann, E. Knoesel, Z. Hu, T. F. Heinz, *Phys. Rev. Lett.* **83**, 1810 (1999).
21. F. M. Zimmermann, X. Pan, *Phys. Rev. Lett.* **85**, 618 (2000).
22. If ψ_L and ψ_R are the wave functions corresponding to the Si-H bonds on the left and right side of the H-filled dimer then the wave function for the entire dimer can be written as $(\psi_L + \psi_R)^2 (\psi_L - \psi_R)^2$, which is odd with respect to reflection across the dimer bond. Because the interaction in the H_2 product is bonding (i.e., even), if symmetry is conserved then the bare dimer produced immediately after desorption must have odd symmetry, representing an excited state of the dimer.
23. T. C. Shen, P. Avouris, *Surf. Sci.* **390**, 35 (1997).

24. We thank W. A. Goddard III and J. E. Northrup for valuable discussions. Financial support for this work was provided by the National Science Foundation under Contract DMR 9812416, and is gratefully acknowledged.

5 July 2000; accepted 21 August 2000

Detection of Daily Clouds on Titan

Caitlin A. Griffith,[1] Joseph L. Hall,[1] Thomas R. Geballe[2]

We have discovered frequent variations in the near-infrared spectrum of Titan, Saturn's largest moon, which are indicative of the daily presence of sparse clouds covering less than 1% of the area of the satellite. The thermodynamics of Titan's atmosphere and the clouds' altitudes suggest that convection governs their evolutions. Their short lives point to the presence of rain. We propose that Titan's atmosphere resembles Earth's, with clouds, rain, and an active weather cycle, driven by latent heat release from the primary condensible species.

Titan possesses an atmosphere often compared to that of Earth. It is composed mainly of N_2, with a surface pressure of 1.5 bar (150 kPa), and possesses a wealth of organic material. Moreover, Titan may support a methane cycle, resembling Earth's hydrologic cycle, with clouds, rain, and seas (*1*, *2*). In the past decade, dozens of images and spectra have been recorded through narrow spectral regions or "windows," where Titan's otherwise optically thick atmosphere is largely transparent. However, no indication was found for the presence of rain and oceans, which are difficult to ascertain by remote measurements. Observations also showed no evidence (*3*–*9*) of clouds (relatively easy to detect), with one exception (*10*).

On 4 and 5 September 1995, spectra recorded within four windows revealed flux enhancements of 14 to 200%, indicative of the presence of a hurricane-sized cloud system (*10*). This first appearance of clouds challenged our understanding of weather on a planetary body similar to, yet intriguingly different from Earth, while providing insufficient data (one event) for its investigation. Compared to Earth, Titan's atmosphere is cooler, more massive, and thus essentially more sluggish. Titan spins slowly, providing little vorticity to cloud systems. In addition, Titan receives ~100 times less power from the sun (Table 1).

To investigate Titan's weather, we recorded repeated observations within three spectral windows. We obtained 21 spectra at 1.8- to 2.4-μm wavelength, 10 spectra at 1.5 to 1.8 μm, and 15 spectra at 2.4 to 3.0 μm in September 1999. These data are supplemented by five spectra from 1993 and 1997 (Table 2). Titan's 1.8- to 2.4-μm albedo (Fig. 1) manifests characteristics of the moon's surface, stratosphere, and troposphere. Prominent flux variations occurred at 2.0 to 2.11 μm, where Titan's atmosphere is most transparent, and result from Titan's surface as different terrains rotate into view (Fig. 1). No variations appeared at 2.17 to 2.4 μm, where sunlight reflects from Titan's stratosphere, which does not observably change over a fortnight. Subtle variations emerged at 2.12 to 2.17 μm, where sunlight penetrates deep into Titan's atmosphere but does not reach the surface. These indicate the presence of variable cloud coverages (*11*).

To better discern the spectral variations, we calculated the difference between each spectrum and that with the lowest 2.11- to 2.17-μm albedo (the second observation of 14 September 1999, spectrum 6b in Table 2). The 2.11- to 2.17-μm flux variations emerge clearly in contrast to the noise at 2.17 to 2.4 μm and the uncorrelated surface variations shortward of 2.11 μm (Fig. 2). Most notably, these flux enhancements consistently occur at ~2.155 μm (Fig. 2). In addition, variations arise in spectra recorded 2 hours apart (Table 2) [Web fig. 1 (*12*)].

The 1.5- to 1.8-μm observations indicate variations consistent with those recorded at 2.11 to 2.17 μm (Fig. 2). Among the noisy 2.4- to 3.0-μm data, only the 22 September

---

[1] Department of Physics and Astronomy, Northern Arizona University, Flagstaff, AZ 86011–6010, USA. [2] Gemini Observatory, Hilo, HI 96720, USA.